The mechanism of radiation damage revealed by EPR, UV-visible microspectrophotometry, and X-ray diffraction studies

(It's worse than you think!)

Edward H. Snell, Kristin A. Sutton, Paul Black, Kermit R. Mercer,
Elspeth F. Garman, Robin L. Owen and William A. Bernhard

X-rays are damaging to Biological Crystals

- Macromolecular X-ray crystallography subjects a crystal to typical X-ray doses on the order of kGy **per image**.
- Multiple images are used to build up a complete data set.
- The LD_{50} for a human (the dose for which 50% of the affected population do not survive) is 4.5 Gy, i.e. 0.0045 kGy

X-rays are damaging to Biological Crystals

- Cryoprotection techniques reduce the rate of radiation damage
- So do the large number of repeating units within a crystal
- However:
  - Structural effects due to radiation damage are more likely to be present in crystals than not.
  - Specific structural damage to particular covalent bonds occurs in a reproducible order.
    - First disulfide bridges elongate and then break,
    - second glutamates and aspartates are decarboxylated,
    - third tyrosine residues lose their hydroxyl group and
    - fourth the carbon-sulfur bonds in methionines are cleaved.

Damage is seen both locally and globally

- Global effects (seen in the diffraction data) include decreasing diffraction intensity increasing B-factor, R-factors, mosaicity and unit cell volume.

- Structural damage has happened before global effects on the diffraction quality are seen.

Solid State Models of Radiation Damage in Biological Systems are Available

- The dose dependence of radiation products from DNA crystals has been studied by in situ X-ray irradiation and Electron Paramagnetic Resonance (Swarts et al., 2007).
- This study showed a transition in the dose rate response at 10-100 kGy.
- A single one-to-one correspondence between radical intermediate and end product could not explain this result.
- In typical X-ray diffraction data collection, a single image is recorded at a dose on the orders of kGy.

In crystallography experiments ‘multitrack’ radiation damage processes may be present

- As the absorbed dose increases the photoelectric effect dominates.
  - This creates a fast electron along with an associated cation.
  - The photoelectron propagates along a track creating additional energetic electrons and cations.
  - The ejected electrons eventually thermalize creating primarily anions.
  - The resulting track is a branched inhomogeneous distribution of anions, cations, and excitations.
- The probability of one track overlapping with another increases and consequently the probability of any given site being ionized twice also increases. radical intermediate and end product – this is termed the Multitrack model.

Three pathways in the damage process

M= parent Molecule

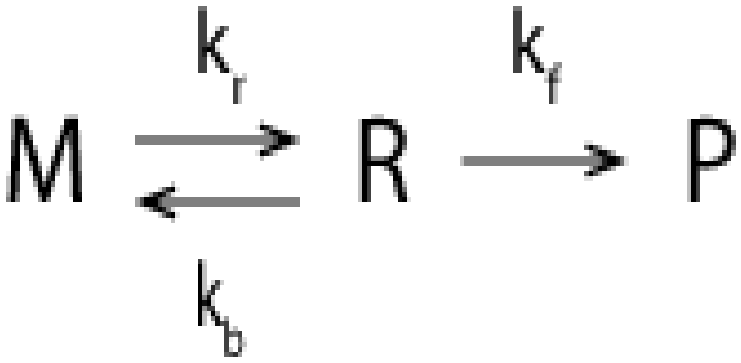

P= Product

R= Radical intermediate

k_r = radical formation
k_b = back reaction
k_f = product formation

Consider only the disulphide bond

A proposed scheme …

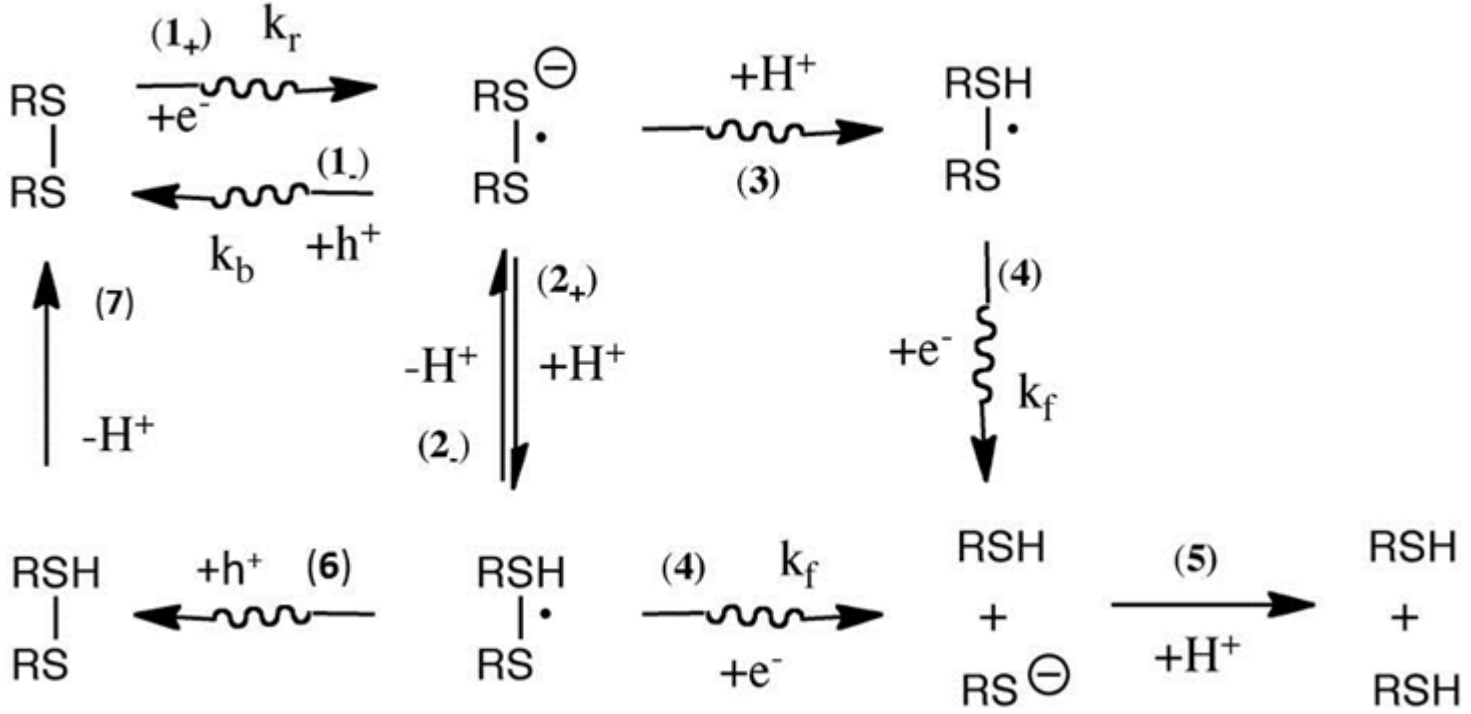

Based on well developed radiation chemistry studies

In step 1+, one-electron addition yields the radical anion, SS•- with the rate constant k_r.

If RSSR is coordinated with a favorable proton donor, then proton transfer gives the neutral radical, SS(H)•, step 2+. This is reversible, with the back reaction indicated as step 2- (a repair pathway).

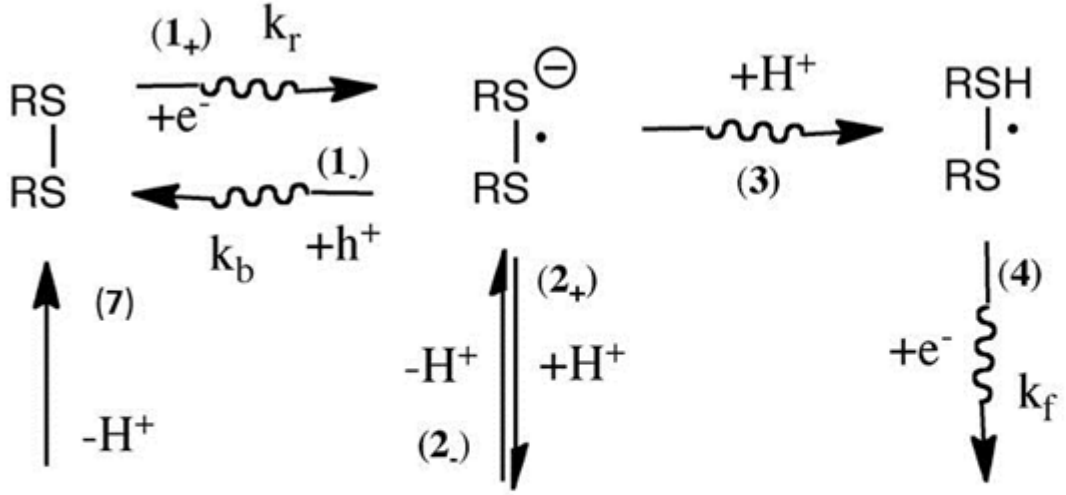

The cleavage products, RSH and RS-, can progress via step 5 to give RSH + RSH. Pivotal to SS cleavage is the competition between the back reaction at rate k_b in 1- and the forward reaction at rate k_f in step 4.

If a radical cation is generated in the proximity of RS-SR, either by the same track or a second track, deprotonation of that radical cation may result in protonation of SS•-: this is presented as step 3. Unlike 2+, step 3 is not reversible. The unpaired electron in SS•- and SS(H)• resides in a three-electron sigma bond.

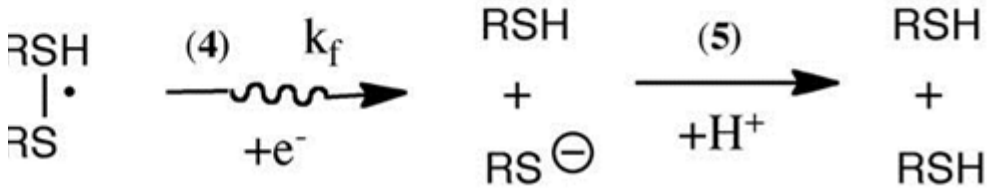

On the other hand, electron attachment (step 4) drives SS(H)• forward to the product, with a rate constant of k_f.

Reaction with a hole generated by the same, or a second track, takes the radical anion backwards to its parent (step 1- in the case of a deprotonated radical or step 6 for the protonated radical species).

How do we study this?

Experiment ….

- Study the process with atomic detail:
  - X-ray crystallography (shows the electron density and loss or gain of electrons)
- Quantitate the chemistry going on
  - Electron Paramagnetic Resonance (measures unpaired electrons, distinct spectrum for different species) with *in situ* irradiation
- Link the two measurements (at very different doses) with UV/visible microspectrophotometry

Use a model protein with disulphide bonds

- Chicken Egg White lysozyme (CEWL).
- Has a history in Radiation Damage Studies
- Four disulphide bonds
- Crystals were grown with a protein concentration ranging from 50-75 mg/ml in pH 4.8 0.1 M sodium acetate buffer.
- The precipitant, also in the same buffer, contained 7.5-15 % sodium chloride and 25 % ethylene glycol as a cryoprotectant agent.
- These were used for X-ray Crystallographic studies and Electron Paramagnetic Resonance
- For the UV/visible spectroscopy (microspectrophotometry) studies, similar crystallization conditions were used with the exception that the cryoprotectant agent was incorporated by soaking crystals in mother liquor containing 20 % (v/v) glycerol.

The choice of model protein is largely unimportant …. in this case

While CEWL crystals are used to test the model, the model itself is based on physical-chemical properties and therefore its application is not limited to lysozyme.

X-ray Crystallography


Not as pretty as Diamond

Experimental detail

- Crystals were flash cooled in liquid nitrogen and diffraction data were collected at 100 K using a MAR325 CCD detector on beamline 9-2 of SSRL.
- The data were collected at an X-ray energy of 12 keV (1.033 Å) and the beam was attenuated by 93.6% giving a flux of 3.8×10^{10} phs^{-1}.
- Two initial images were recorded 90° apart and these were used to define an appropriate starting angle.
- A total of 15 datasets over 57° were collected using a 2 s exposure and oscillation angle of 1°, each data set starting at the same position as the first ensuring that the same area of the crystal was irradiated during each dataset.
- The crystal was approximately 0.3 x 0.3 x 0.3 mm with the beam (approximating a top hat profile) illuminating an area of 0.2 x 0.2 mm.
- The absorbed dose was estimated using the program RADDOSE, but not adjusted for fresh regions of the crystal that rotated into the beam (estimated to reduce the calculated absorbed dose by less than 0.2% per °).

Absorbed dose

Data sets	15
Absorbed dose per data set	0.07 MGy
Total dose	1.05 MGy

X-ray Crystallographic Data

- The data were integrated with HKL2000 and reduced with SCALA.
- An initial model molecular model was refined against the data using PHENIX and manual model building with COOT.
- The process continued until there were no unexplained positive or negative peaks in the electron density above 5 sigma.
- Isomorphous difference Fourier maps, Fo_n-Fo_1 were calculated the observed amplitudes from each dataset and the phases derived from model fitted to the first dataset.
- The solvent accessibility of the cysteine residues involved in the disulfide bonds was calculated using AREALMOL.

X-ray Data Refinement

Data collection statistics				
	First data set	Last data Set	Mean	Standard deviation
Cell param. (a=b, c Å)	78.77, 36.86	78.77, 36.87	78.76, 37.39	0.006, 0.004
Wilson B factor Å^2	10.67	11.32	11.12	0.163
Structural statistics				
R_{work}/R_{free} (%)	19.09/19.97	19.12/20.30	19.14/20.31	0.128/0.273
SS bond length (Å)				
Cys 6 - Cys 127	2.04	2.05	2.04	0.0051
Cys 30 - Cys 115	2.05	2.09	2.09	0.0139
Cys 64 - Cys 80	2.04	2.05	2.04	0.0046
Cys 76 - Cys 94	2.02	2.04	2.03	0.0077

•Crystallographic data and structural refinement statistics for a lysozyme crystal from which structural X-ray data were collected. The absorbed dose for each data set was 0.07 MGy with 15 data sets giving a total absorbed dose of 1.05 MGy.

Disulphide bonds

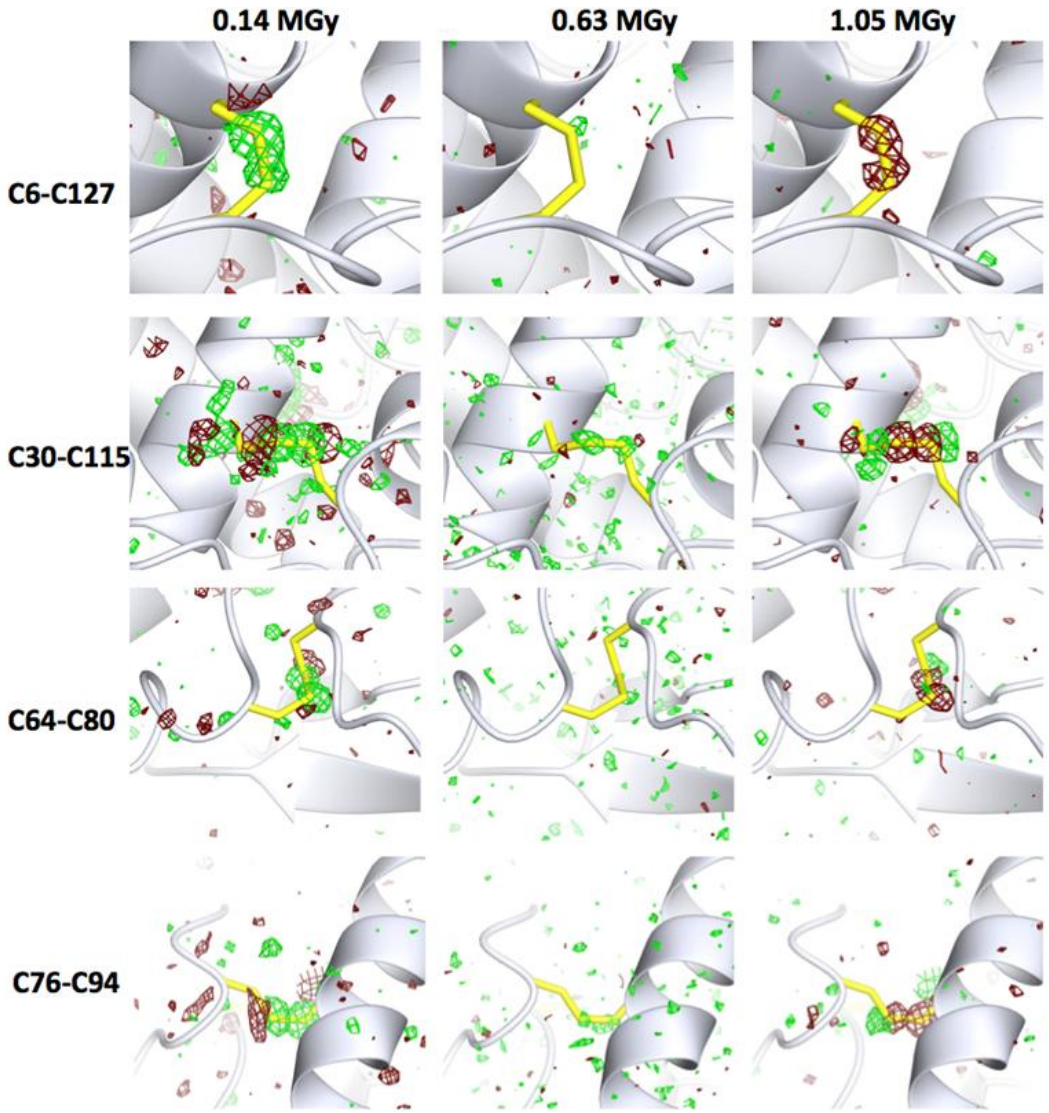

Isomorphous difference density maps Fo_n-Fo_1 (where n is the data set number) around the four disulfide bonds present in lysozyme.

Maps are shown for Fo_2-Fo_1 (0.14 MGy), Fo_9-Fo_1 (0.63 MGy) and Fo_{15}-Fo_1 (1.05 MGy).

Disulfide bonds are highlighted in yellow.

Maps are contoured at +3σ (green) and -3σ (red).

For C6-C127 the top most part of the bond is C6 with the bottom being C127. The remaining bonds are positioned such that the label matches the residue positions in each figure with the first to the left and the second to the right. Note that the dose indicated is the cumulative dose.

Methionine residues as a control

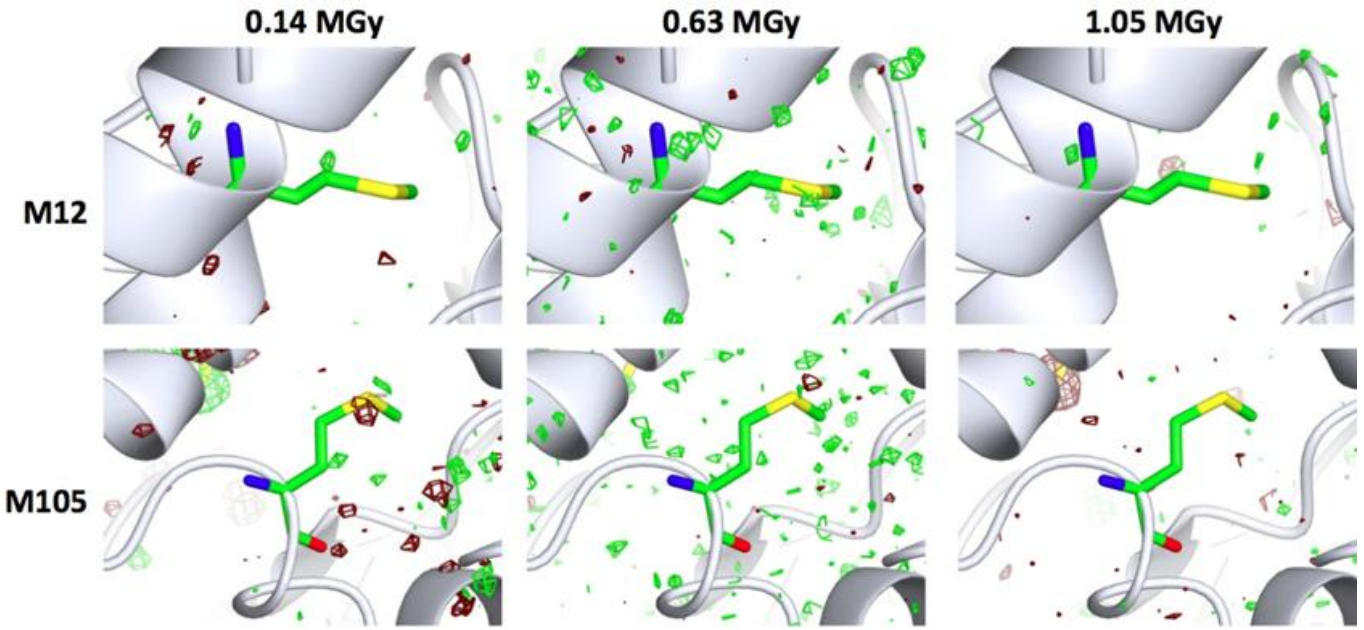

Isomorphous difference density maps Fo_2-Fo_1 (0.14 MGy) Fo_9-Fo_1 (0.63 MGy) and Fo_{15}-Fo_1 (1.05 MGy) for residues Met12 and Met105. Maps are contoured at 3σ in green and -3σ in dark red.

Electron Paramagnetic Resonance

Electron Paramagnetic Resonance

- Electron spins are excited.
- Electron pairs do not produce signals
- Unpaired electrons do
- Sensitive to free radical formation

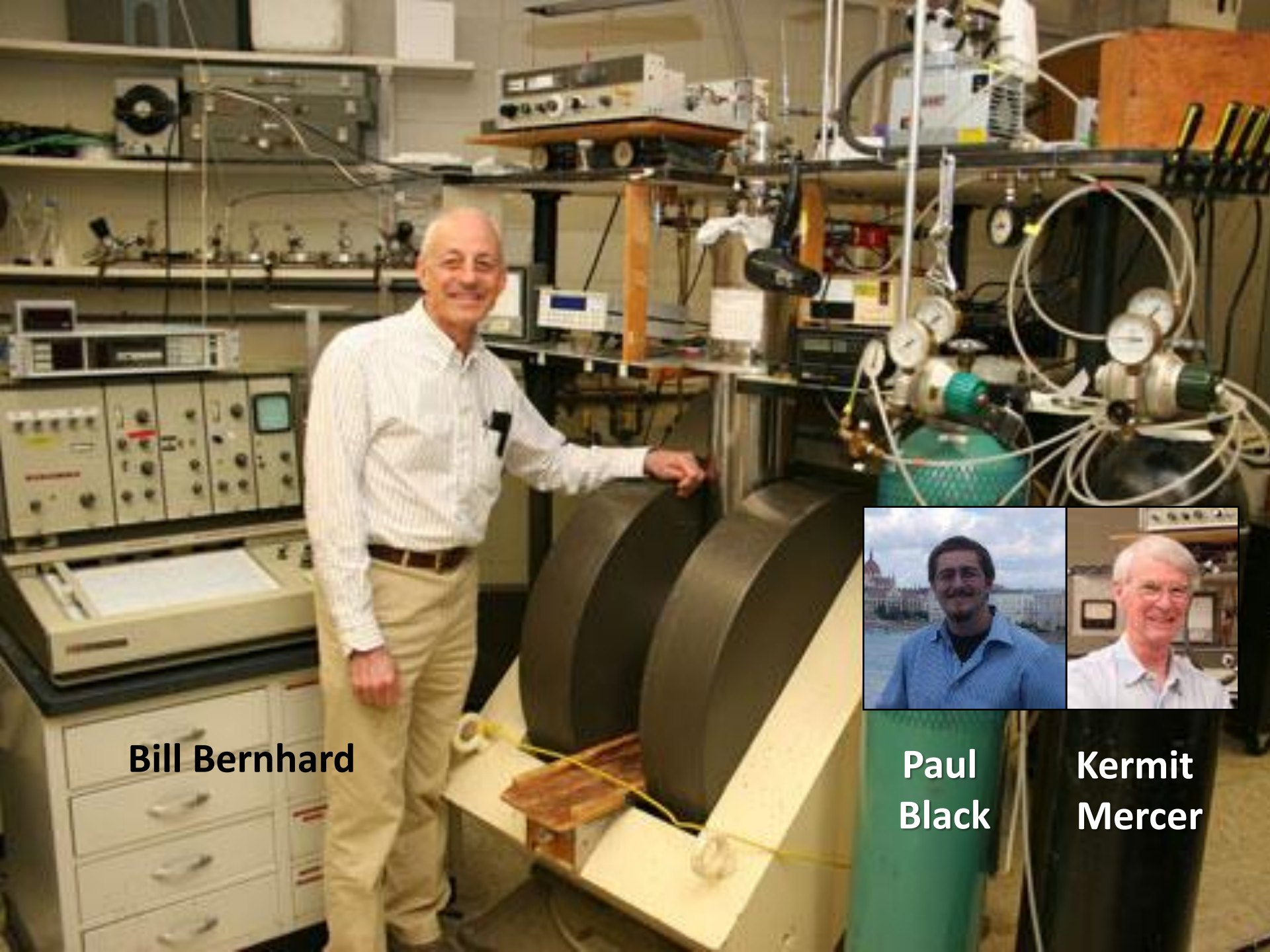
Bill Bernhard
Paul Black
Kermit Mercer

Experimental data collection

	Dimensions (mm)	Volume (mm^3)$^+$	Weight (µg)	Dose points for EPR measurements (kGy)
Crystal 1	0.60 × 0.50 x 0.40	0.12	208	5, 10, 20, 40, 60, 100, 150
Crystal 2	0.50× 0.50 x 0.25	0.06	135*	10, 20, 40, 60, 100
Crystal 3	0.50× 0.50 x 0.40	0.10	185*	20, 40, 100, 200, 300, 400, 500

Volume is approximate, calculated by assuming a cuboid which does not take into account crystal shape. *Masses were calculated based on the measured radical yield at a dose of 20.

EPR Experimental Setup

- Crystals mounted in 1.0 mm outer diameter thin walled quartz glass capillaries
- Inserted one at a time into a Janis liquid helium cryostat in the EPR instrument and cooled to a temperature of 4 K in less than 30 seconds (the cryostat maintains temperature through expansion of liquid helium into a vacuum environment).
- No attempt was made to obtain precise information on the alignment of the crystals with respect to the magnetic field.
- Crystals were irradiated in situ with median energy 50 keV X-rays at 4 K using a Varian/Eimac OEG-76H tungsten target tube operated at 70kV, 20 mA, and filtered by a 25 µm aluminum foil.

Crystalline ice, if present, is not a problem

- Dose rate at the sample was 0.0125 kGy s^{-1}, determined by calibration with radiochromic film .
- Following irradiation, EPR data collection was performed on samples at 4 K. First-derivative EPR-absorption spectra were recorded at Q-band (35.3 GHz) microwave frequency.
- Ice irradiated at 4 K gives a distinctive 50 mT doublet Lack of the doublet showed ice content lower than a few percent of crystal mass : the cooling procedure used created little to no water ice.
- Note that the EPR signal is largely independent of ice type (Bednarek et al., 1998) so unlike during crystallographic studies, the type of ice formed does not impact the measurements.

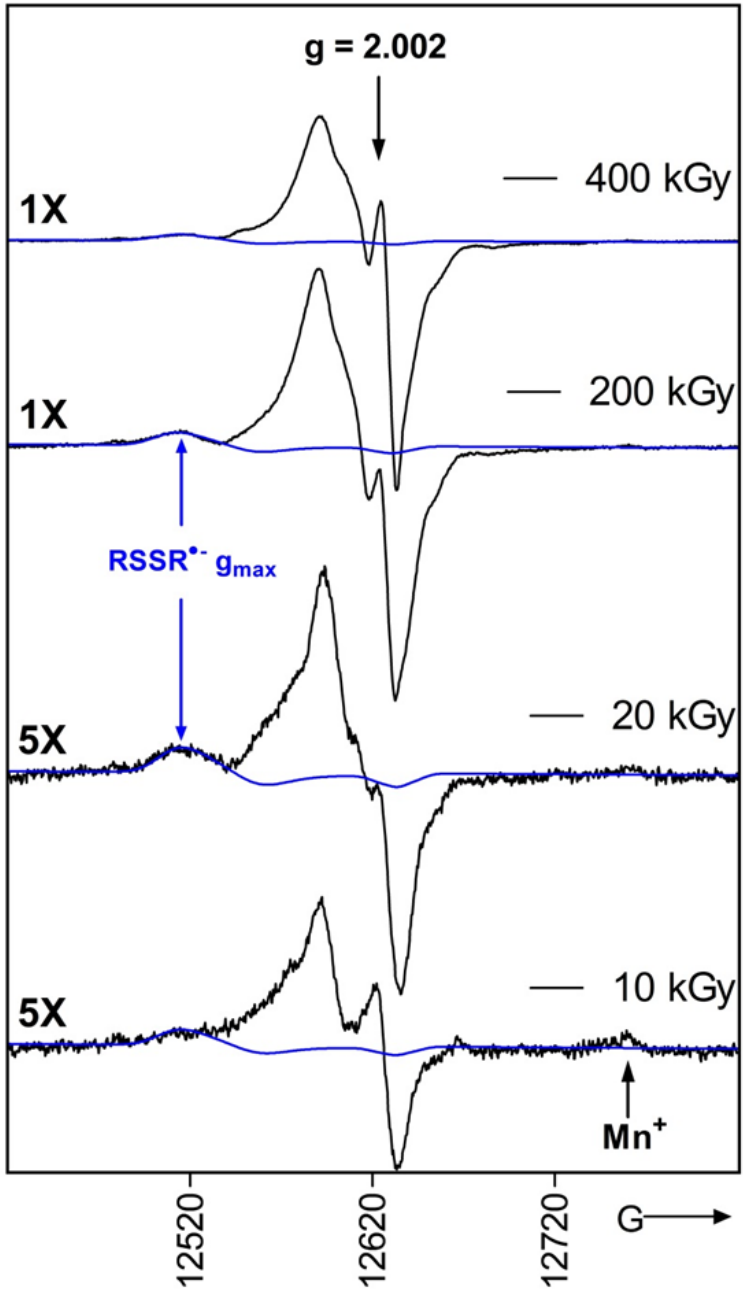

- EPR spectra are shown for four different X-ray doses.
- At low doses in the EPR experiment, e.g., between 10 kGy and 20 kGy, the spectrum intensity increases linearly with dose.
- At higher doses, e.g., 200 kGy to 400 kGy, a plateau is reached.
- The blue traces in Figure 4 are simulations of the RSSH• component, is associated with the low field signal assigned exclusively to RSSH•.
- The double integral of the experimental and calculated spectra gave the radical concentrations, R(tot) and R(SS) respectively. The peak from the growing RSSH• component is indicated along with a peak from trace amounts of Mn+ known to be present in the experimental setup.

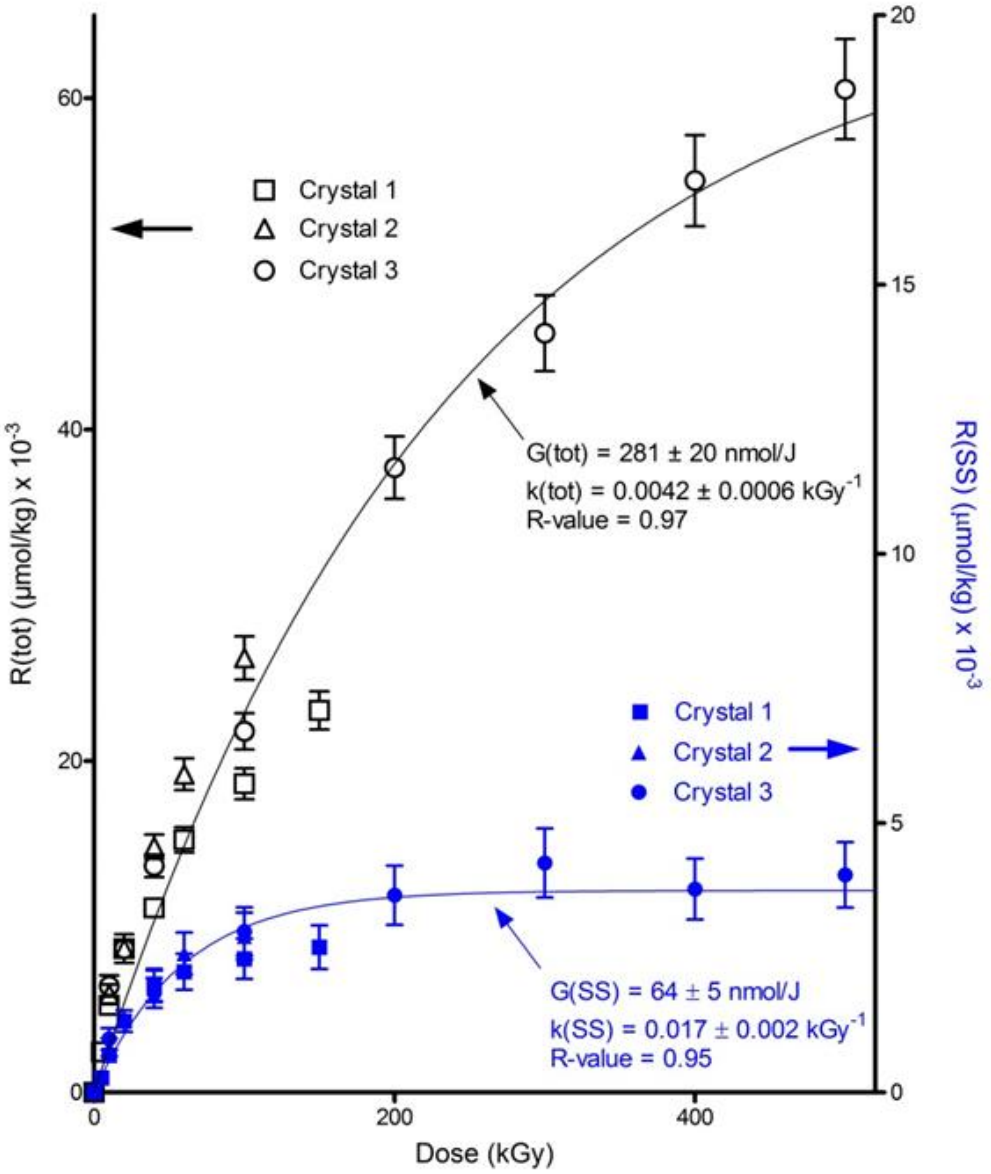

The R(tot) data are plotted using black symbols and the R(SS) data are plotted using blue symbols

The curves fitting these data are derived from a non-linear least squares fit to Equation 6.

The fitting parameters for R(tot) were G(tot) = 281 ± 20 nmolJ-1 and k = 4.2 ± 0. 6 MGy-1.

For R(SS), the fitting parameters were calculated to be G(SS) = 64 ± 5 nmolJ-1 and k = 17 ± 2 MGy-1.

Saturation values for R(SS) vs. R(tot) are distinctly different, reflecting the differences in dose response properties between the radical species. R(SS) saturates ~ 200 kGy at a value of $R(SS)_\infty$ = 3.7 ± 0.5 mmol kg-1, whereas R(tot) saturates above 500 kGy at a value of $R(tot)_\infty$ = 66 ± 10 mmol kg-1.

This difference is a consequence of the relatively large destruction cross-section for the SS centered radicals compared to those of the other radical species trapped in lysozyme.

UV/visible microspectrophotometry measurements

Diamond Light Source

Elspeth Garman

Robin Owen


Diamond
setup on I24

UV/visible microspectrophotometry

- Eight crystals were mounted in nylon loops and held at 100 K.
- They were irradiated with X-rays of energy 12.8 keV with the beam was defocused to 50×50 μm^2
- Incident fluxes ranging from 8.58×10^9 ph s-1 to 1.54×10^{12} ph s^{-1} at the sample position (filter transmission from 0.8% to 100%) - dose-rates ranging from 1.5 to 2700 kGy s^{-1}.
- Crystals were subjected to a single X-ray exposure, the duration of which varied such that the total absorbed dose was ~5 MGy.
- Changes in UV/visible optical absorbance were measured using an in-situ microspectrophotometer with a 50 µm diameter probe beam to closely match the X-ray illuminated area.

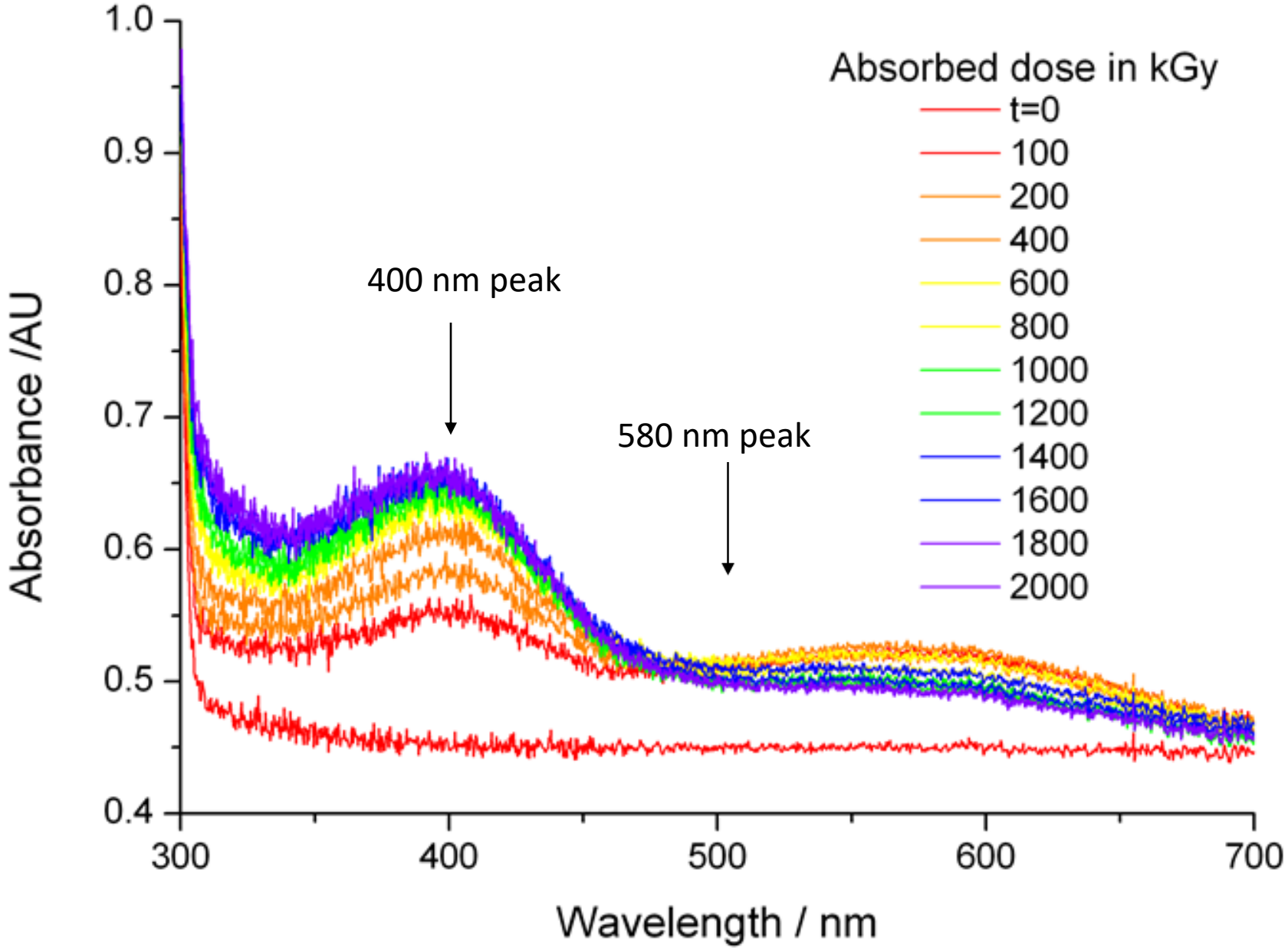
Absorbance /AU
1.0
0.9
0.8
0.7
0.6
0.5
0.4
300
400
500
600
700
Wavelength / nm
400 nm peak
580 nm peak
Absorbed dose in kGy
t=0
100
200
400
600
800
1000
1200
1400
1600
1800
2000

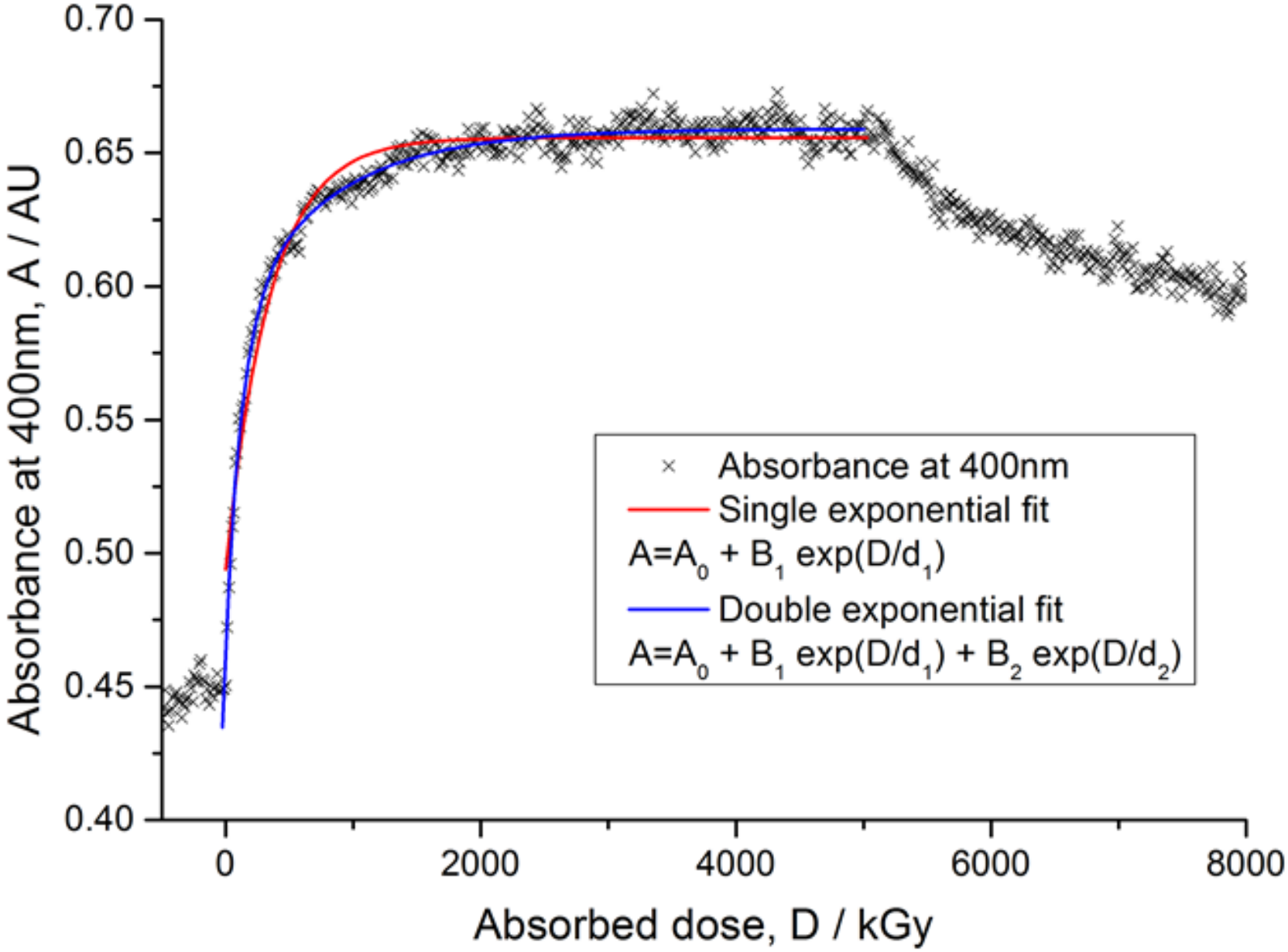
0.70
0.65
0.60
0.55
0.50
0.45
0.40
Absorbance at 400nm, A / AU
0
2000
4000
6000
8000
Absorbed dose, D / kGy
Absorbance at 400nm
Single exponential fit
A=A0 + B1 exp(D/d1)
Double exponential fit
A=A0 + B1 exp(D/d1) + B2 exp(D/d2)

For all 8 crystals …

- The dose response curves were fitted to both a single and a double exponential function

$$Abs = A_0 + B_1 e^{(D/d1)} + B_2 e^{(D/d2)}$$

where A_0 is the baseline, B_1, B_2, d1 and d2 are constants, and D is the dose.

- All data could be well fitted with a single or double exponential with an $R^2 \geq 0.95$, although visual inspection of fits showed that the double exponential fit better describes the data for all crystals.
- We define the saturating dose, D90, as the point at which the absorbance reaches 90% of the maximum above baseline (where fast changes no longer dominate).

Crystal	Attenuation (%)	Flux (ph s^{-1})	Dose rate (kGy s^{-1})	D_{90} single (kGy)	D_{90} double (kGy)
1	0	1.51×10^{12}	270	772	921
2	0	1.34×10^{12}	240	451	557
3	48.0	6.78×10^{11}	121	465	376
4	73.0	3.45×10^{11}	62	711	928
5	90.0	1.08×10^{11}	19	289	533
6	96.0	4.67×10^{10}	8.4	541	1183
7	98.2	1.99×10^{10}	3.5	482	819
8	99.2	8.58×10^{9}	1.5	461	716
		Average		521	771

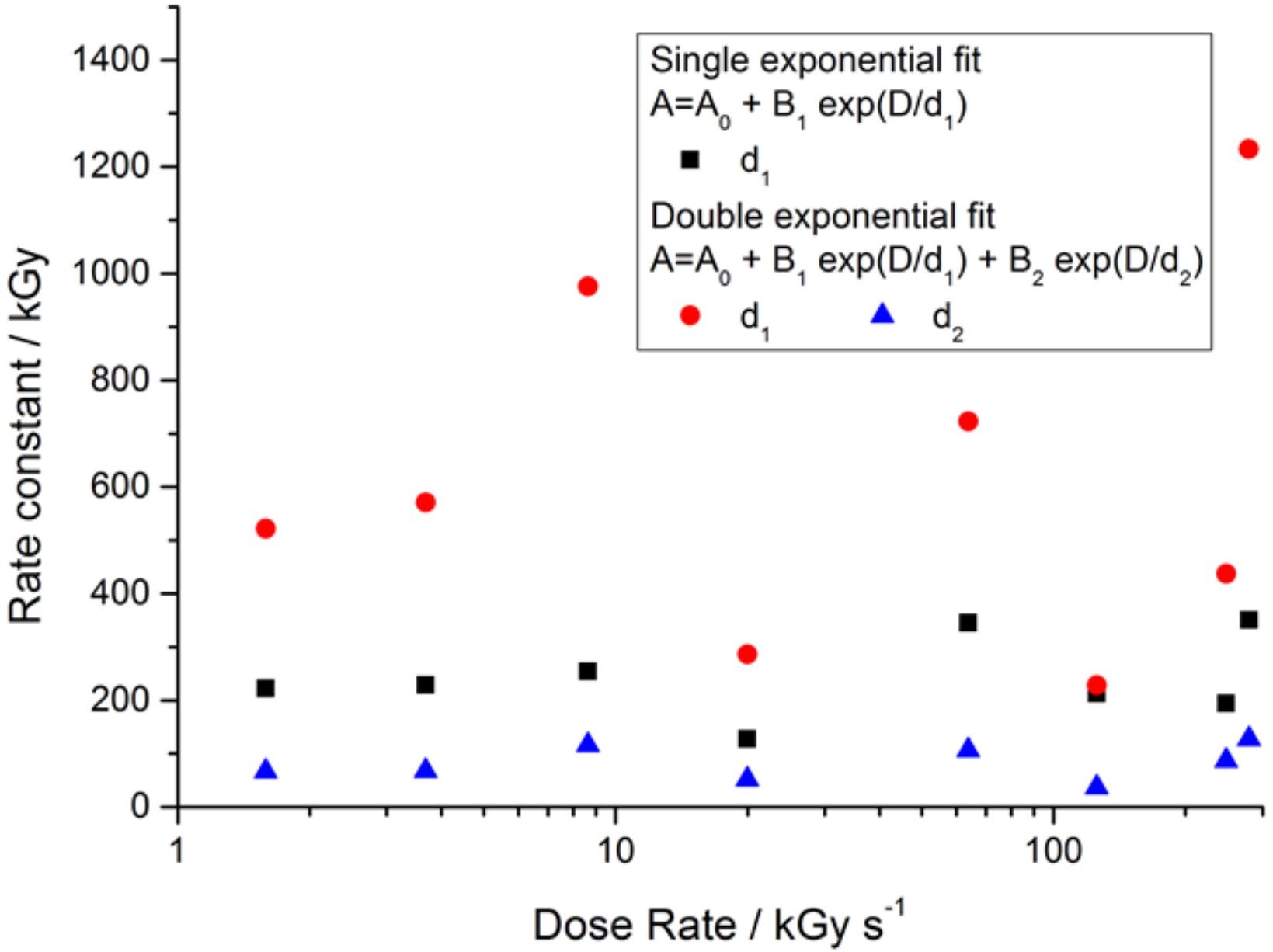
Single exponential fit
A=A0 + B1 exp(D/d1)
d1
Double exponential fit
A=A0 + B1 exp(D/d1) + B2 exp(D/d2)
d1
d2
Rate constant / kGy
Dose Rate / kGy s-1
0
200
400
600
800
1000
1200
1400
1
10
100

Multiple exposure with a rest period

- The change in absorbance from a series of 1 s exposures interspersed with a 5 s rest period
  - Despite a rapid reduction in absorbance when the X-ray shutter was closed for the rest period, saturation at 400 nm was still achieved rapidly with a progressively smaller change in absorption for the same additional absorbed dose.
  - The reduction in absorption seen during the rest period indicates that some fraction of SS•- was lost due to recombination and/or protonation, but the dominating increase over time indicates that some fraction was stable

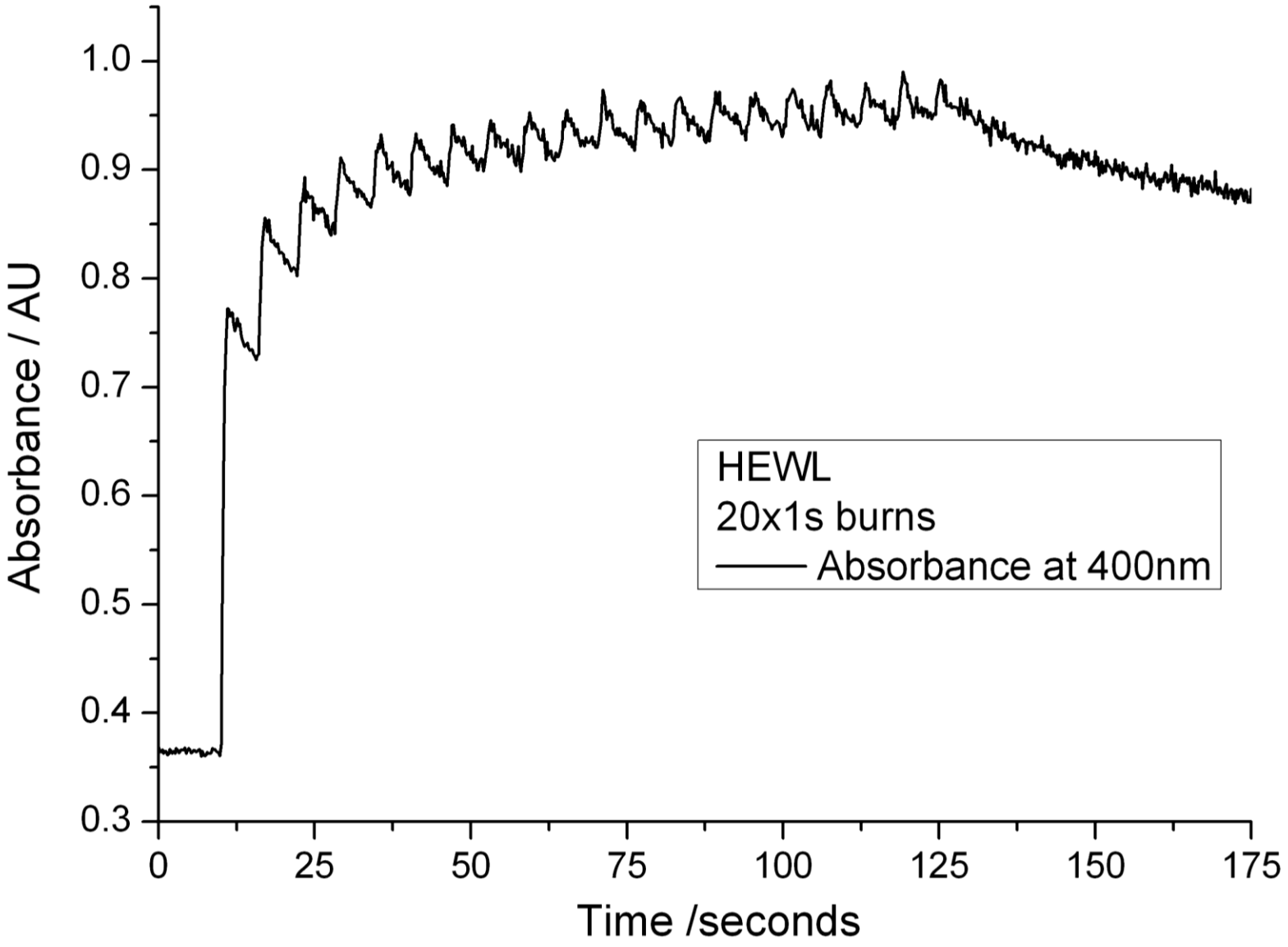
Absorbance / AU
1.0
0.9
0.8
0.7
0.6
0.5
0.4
0.3
0
25
50
75
100
125
150
175
Time /seconds
HEWL
20x1s burns
Absorbance at 400nm

Decay of Signal

- A 20 s continuous X-ray exposure.
- The post-exposure decay of the disulfide peak at 400 nm was monitored.
- The decay follows a double-exponential decay with rate constants of d1 and d2 equal to 13.1 ± 1.6 and 140.2 ± 20.7 s-1 respectively.
- The fit of the decay by a double exponential function is in agreement with previous observations (Owen et al., 2011, Beitlich et al., 2007)

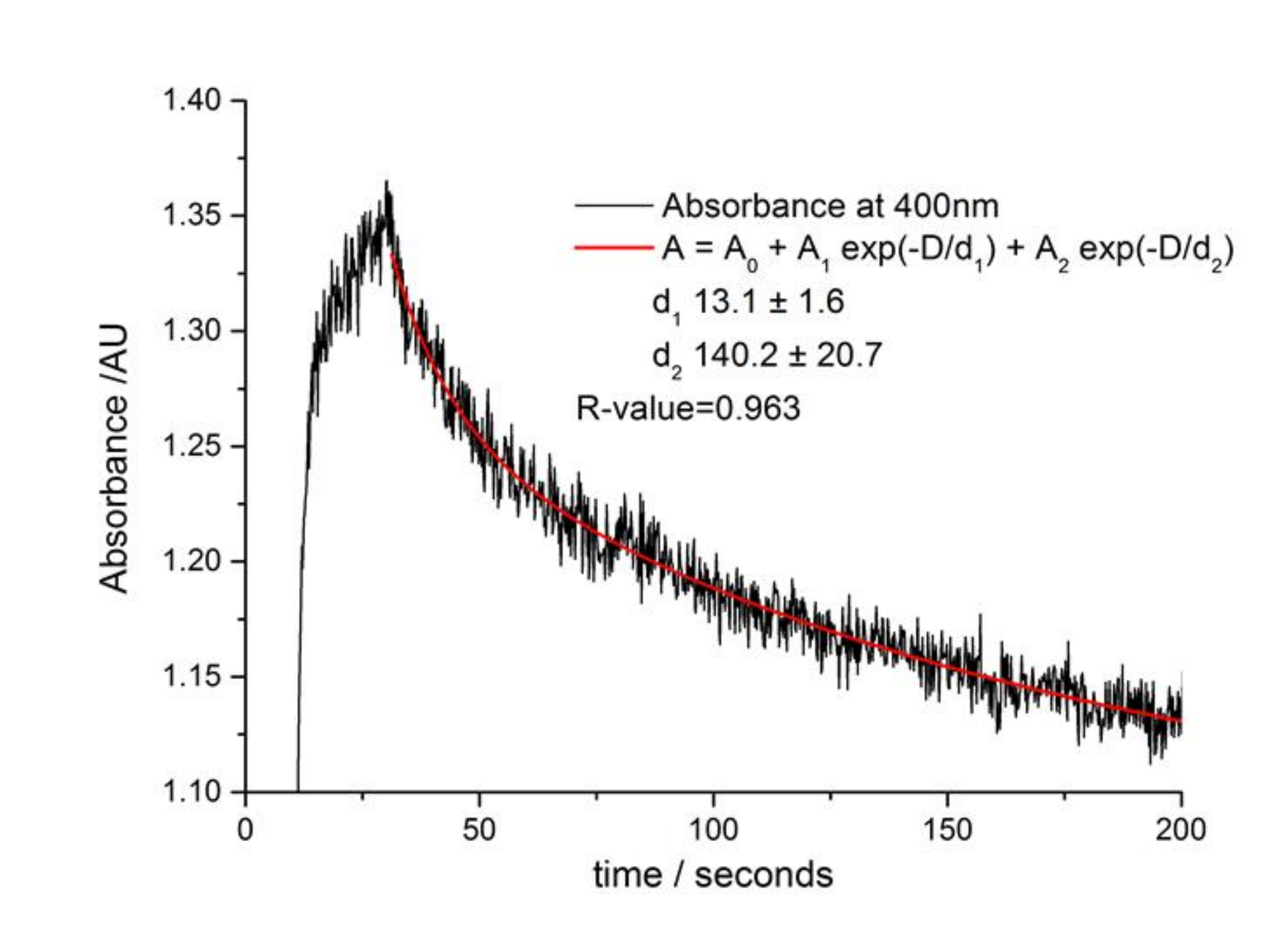
Absorbance at 400nm
A = A0 + A1 exp(-D/d1) + A2 exp(-D/d2)
d1 13.1 ± 1.6
d2 140.2 ± 20.7
R-value=0.963
Absorbance /AU
time / seconds
1.40
1.35
1.30
1.25
1.20
1.15
1.10
0
50
100
150
200

UV/visible microspectrophotometry results

- The increased absorbance at 400 nm is attributable to the radical species SS•- and an increase in absorbance at this wavelength was clearly observed in all samples.
- This was accompanied by a peak in absorption at ~580 nm attributable to the formation of solvated electrons.
- Both of these features can clearly be seen in the spectral series which shows the results of a continuous 80 s irradiation with a cumulative dose of 5 MGy (dose rate 62 kGy s-1).
- Absorbance at 400 nm increases rapidly before saturating and the 580 nm peak due to solvated electrons has an observed maximum at the earliest recorded point.
- This peak may have been higher at earlier time points (below 200 ms) that were not captured in the experiment.

Bringing it all together

Results

- UV/visible spectroscopy showed that disulfide radicalization appeared to saturate at an absorbed dose of approximately ~0.5-0.7 MGy (depending on the fit).
- In contrast to a saturating dose of ~0.2 MGy observed by EPR at a much lower (in the largest case a factor of 216,000) dose rate.
- That saturation occurs in both cases suggests that a multi-track model involving product formation due to the interaction of two separate tracks, is valid.

- Our model fits well across a range of X-ray doses, explaining the data from 5 kGy to 1.05 MGy (EPR and crystallographic) and the microspectrophotometry data up to ~5 MGy.
- At even the smallest absorbed dose in our range, (5 kGy), the EPR measurements indicate complete dose saturation of one-electron reduced disulfide bonds within the protein. In addition, our model predicts that the initial reduction of disulfide bridges would not result in the scission of the bond.
- In our study, only the Cys94 of the C76-C94 disulfide bond forms an alternate conformation. Of the two cysteines making up this bond, Cys94 has the lower water accessibility but Cys76 does not show evidence of developing different conformations. The production of a rotamer cysteine could be an indication that cysteine is the major and perhaps only product.
- The disulfide bond with the highest solvent accessibility, C6-C127, shows no evidence of developing any alternate conformation. It would appear that structural perturbation due to ongoing radiation chemistry is both dose and environment specific.

- Even at the lowest doses used for structural investigations, disulfide bonds are already becoming radicalized.
- Extra electron density is present, which if not taken into account, could give misleading results when trying to quantitate damage observed from difference map techniques.
- Practically, there are few ways to avoid this.
- Our model allows us to understand the nature of disulfide bond loss in lysozyme crystals, and can potentially be extended to predict the labiality of each amino acid side chain within a protein.
- More work is required to empirically test this protein damage model, in which other local factors should also be considered, such as solvent accessibility and proximity of other amino acid side chains, all of which are a consequence of secondary and tertiary protein.

Summary

- Understanding radical destruction as well as formation is key to understanding the radiation induced changes that impact X-ray diffraction data.
- A multi-track model involving both formation and destruction has been shown here to be valid in explaining X-ray induced disulfide bond damage, since it fits UV/Visible, EPR and both low and high dose crystallographic data.
- Multi-track considerations offer the first step in a comprehensive model of radiation damage that could potentially lead to a combined computational and experimental approach to identify when damage is likely to be present, to quantitate it, and provide the ability to recover the native unperturbed structure.
- Intriguingly, a successful model would not only allow treatment of new structural information but, in cases where absorbed dose has been recorded, allow identification and potential remediation of previously deposited structural data.

The Workers

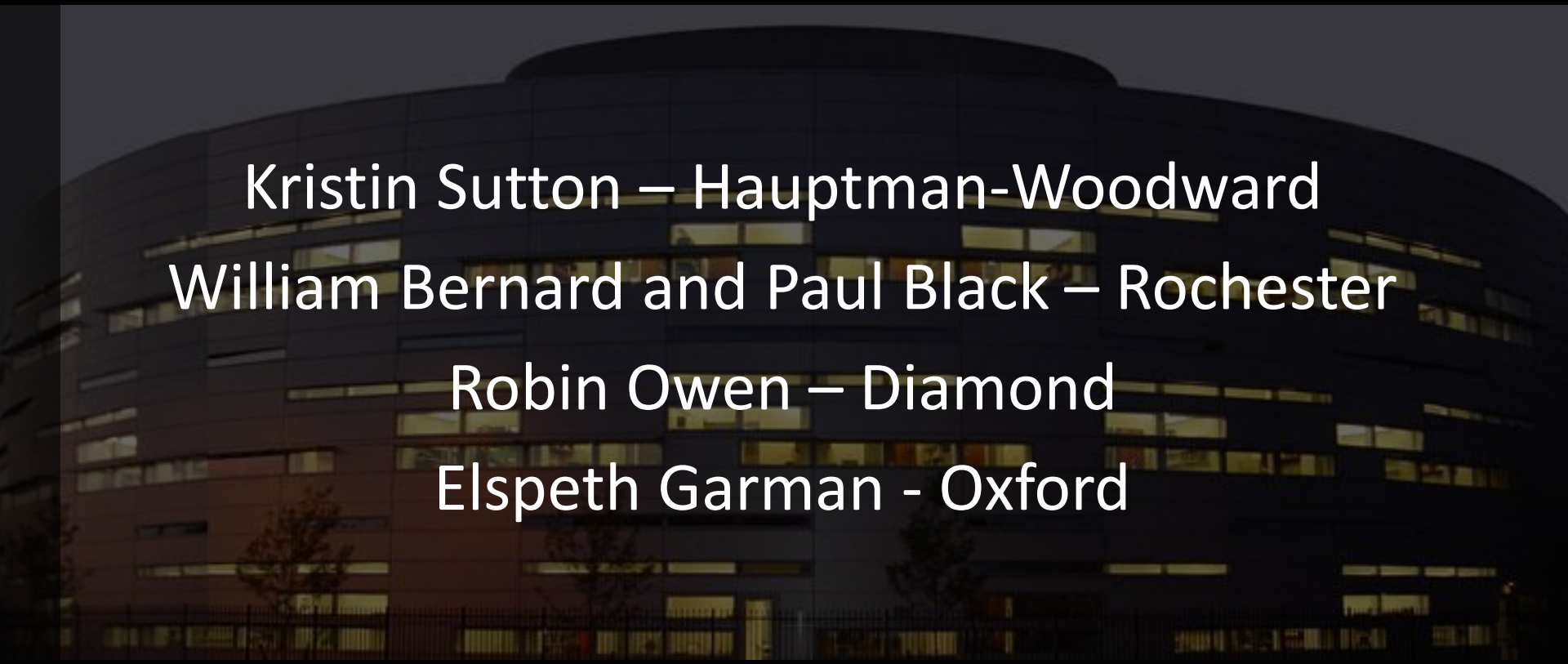

Kristin Sutton – Hauptman-Woodward

William Bernard and Paul Black – Rochester

Robin Owen – Diamond

Elspeth Garman - Oxford

Thank you and questions?

esnell@hwi.buffalo.edu